

Materials Research Express



PAPER

Enhanced hardness of nickel coating reinforced functionalized carbon nanomaterials via an electrodeposition technique

RECEIVED
18 April 2019

REVISED
20 May 2019

ACCEPTED FOR PUBLICATION
29 May 2019

PUBLISHED
5 June 2019

Tran Van Hau^{1,3}, Pham Van Trinh^{1,4}, Nguyen Phuong Hoai Nam³, Vu Dinh Lam², Phan Ngoc Minh² and Bui Hung Thang^{1,2,4}

¹ Institute of Materials Science, Vietnam Academy of Science and Technology, 18 Hoang Quoc Viet Str., Cau Giay Distr., Hanoi, Vietnam

² Graduate University of Science and Technology, Vietnam Academy of Science and Technology, 18 Hoang Quoc Viet Str., Cau Giay Distr., Hanoi, Vietnam

³ VNU University of Engineering and Technology, 144 Xuan Thuy Str., Cau Giay Distr., Hanoi, Vietnam

⁴ Authors to whom any correspondence should be addressed.

E-mail: trinhpv@ims.vast.vn and thangbh@ims.vast.vn

Keywords: graphene, carbon nanotubes, electrodeposition, Ni coating, microstructure, microhardness

Abstract

In this paper, the nickel (Ni) coatings reinforced carbon nanomaterials including graphene nanoplatelets (GNPs), multi-walled carbon nanotubes (MWCNTs) and MWCNTs/GNPs hybrid material prepared by the electrodeposition technique were investigated. GNPs and MWCNTs were functionalized with carboxylic (–COOH) function groups (GNPs–COOH, MWCNTs–COOH) then uniformly dispersed into Watts solution for the electrodeposition process. The obtained results revealed that the microhardness of the Ni coating reinforced COOH functionalized carbon nanomaterials is much improved compared to the bare Ni coating and Ni coating containing carbon nanomaterials without functional groups. The Ni coating containing MWCNTs–COOH/GNPs–COOH hybrid material showed the highest hardness value of 270 HV that is higher 44.7% compared to the bare Ni coating. The enhancement was attributed to the uniform dispersion of functionalized carbon nanomaterials in Ni matrix, the synergistic strengthening effect of the MWCNTs and GNPs, the grain refinement of Ni matrix and the enhanced load transfer effect from Ni matrix to MWCNTs and GNPs via atomic bonding during the electrodeposition process.

1. Introduction

Because of the improvement in mechanical properties compared to the ordinary metallic coating, nanocomposite coatings used for protecting the metallic surface have been receiving the great attention of scientists [1–4]. Many studies have shown that the Ni coating reinforced nanomaterial components has higher hardness and higher anti-corrosion than those of the bare Ni coating [5–7].

The development of science and technology led to the discovery of the new nanostructured materials, which have unique properties. In 2004, Novoselov *et al* discovered graphene (Gr) which has extraordinary mechanical properties [8]. Gr was evaluated as the ‘strongest material ever’ with the sustaining breaking strengths of 42 N m^{-1} , the intrinsic mechanical strain of $\sim 25\%$ and Young’s modulus of 1.0 TPa [9, 10], the large surface area of $2630 \text{ m}^2 \text{ g}^{-1}$ [11]. Carbon nanotubes (CNTs) discovered by Iijima in 1991 were also considered as a super material with the Young modulus from 0.963 to 1.025 TPa for single wall CNTs [12], the Young modulus from 0.126 to 0.937 TPa and the shear modulus from 33 to 875 MPa for the Multi-walled CNTs (MWCNTs) [13]. Because of these properties, Gr and CNTs have been attracting great attention for using the materials as the reinforcements for the metallic coating. Many studies were used CNTs as a reinforcement material, which exhibited a significant enhancement in the hardness, corrosion resistance, wear resistance of the metallic coating [1, 2, 5, 6]. In 2013, Kumar *et al* used graphene oxide (GO) to fabricate Ni–Gr nanocomposite coating. The obtained results have demonstrated the improvement in microhardness and corrosion resistance of the nanocomposite coating [14]. Algul *et al* expanded the study on the effect of Gr concentration on the structure,

Table 1. Watt solution.

Chemicals	NiSO ₄ ·6H ₂ O	NiCl ₂ ·6H ₂ O	H ₃ BO ₃	SDS
Concentration (g ⁻¹)	300	50	40	0,1

microhardness and tribological properties of the nanocomposite coating [15]. B Szeptycka *et al* investigated the effect of Gr concentration on the corrosion resistance and reported that the Ni–Gr coatings have higher corrosion resistance than bare Ni coating [16]. In recent years, several studies have focused on using GO fabricated by Hummer method for the Ni coating via electrodeposition technique. Jabbar *et al* reported the effect of temperature in the electrodeposition method to the surface morphology and the corrosion resistance of Ni–Gr coating [17]. The obtained results demonstrated that the Ni–Gr composite coating fabricated at the temperature of 45 °C have high carbon content, refining grain sizes, high microhardness, and better corrosion resistance [17]. Singh *et al* investigated the tribological properties of Ni–GO composite coating fabricated by pulsed electrodeposition method [18]. The authors reported that the incorporation of GO into the Ni matrix improved both frictions and wear behaviors of the composite coating compared to the bare Ni coating [18]. The mentioned studies on Ni coating using GO prepared by Hummer method have some limitations such as complicated experiments, wasting time and chemicals, and low-quantity samples [19–23].

Thus, in this work, we present a simple method to fabricate the Ni coating reinforced carbon nanomaterials including GNPs and MWCNTs and MWCNTs/GNPs hybrid materials. The influence of carbon nanomaterials and their surface functional state with a carboxyl (–COOH) group on the microstructure, composition, and microhardness of the coatings were investigated and presented.

2. Method

2.1. Materials

GNPs (>99% purity) prepared by plasma exfoliation with the thickness in a range from 2–10 nm and the diameter of 2–7 μm were purchased from ACS Materials, USA. Lab-made MWCNTs (97% purity) were fabricated by the thermal chemical vapor deposition method with the Fe/CaCO₃ catalytic materials, which have 5–15 μm in length and 10–30 nm in diameter [24]. C1220 copper (Cu > 99.90%) was used as a substrate material for the coating process. Other chemicals purchased from Merck & Co., Inc. were used without further purification.

2.2. Preparation GNPs–COOH and MWCNTs–COOH

GNPs were functionalized with the –COOH functional groups using the strong oxidizing agents via three steps. Firstly, GNPs were treated with the mixture of acid HNO₃ and H₂SO₄ with 1/3 (v/v) fraction at a temperature of 70 °C for 5 hours to attach COOH functional groups on the surface of Gr. Secondly, the solution was filtered and washed by distilled water for few times to remove the residual acids. Finally, the obtained solution was filtered by using a 200 nm cellulose nitrate membrane to obtain GNPs–COOH. MWCNTs–COOH were prepared using the same process for GNPs–COOH.

2.3. Preparation of plating solution

Watts solution was prepared using the components as shown in table 1. Sodium dodecyl sulfate (SDS) surfactant was added to enhance the wetting for electrodes. As-received GNPs, as-received MWCNTs, GNPs–COOH, and MWCNTs–COOH were dispersed into a liter Watt solution with a designed concentration as shown in table 2. The received solutions were ultrasonicated for 60 min to obtain the homogeneous Watt solutions for the electrodeposition process.

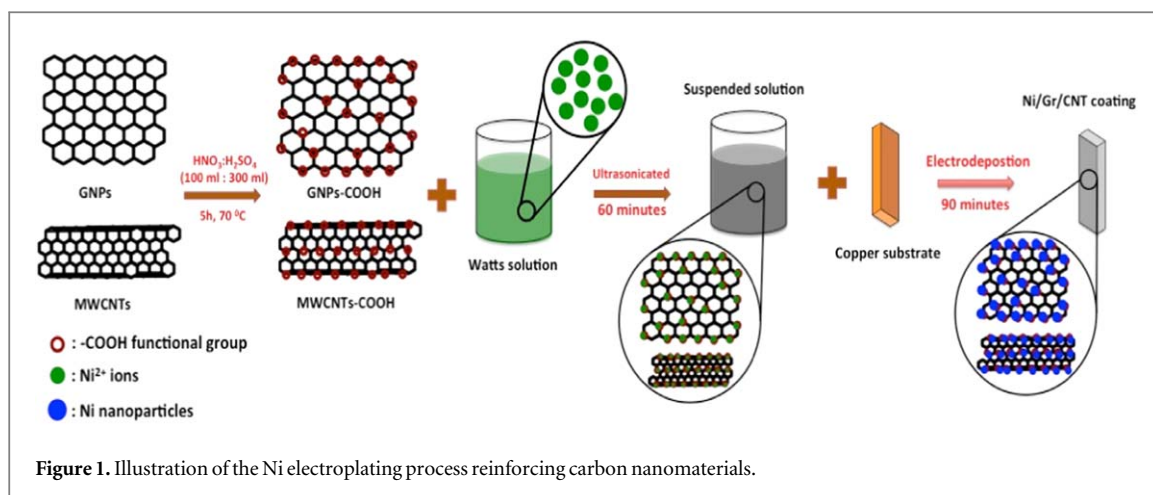
2.4. Electrodeposition process

The electrodeposition process for Ni coatings reinforced carbon nanomaterials is described in figure 1. The copper substrate with a size of 40 × 50 × 1 mm was treated with two main steps. Firstly, copper substrates were ground by the sandpaper with the different grit sizes then polished by alumina powder. Secondly, the polished copper substrates were cleaned by acetone, isopropanol, and distilled water respectively in an ultrasonication bath for 30 min to remove the residual organics.

The electrodeposition process of Ni and Ni reinforced carbon nanomaterials were performed with the electrodeposition equipment that has a 3-electrodes system in which there is a cathode located between two anodes. Anodes are made of pure Ni with the size of 40 × 50 × 5 mm and the copper substrate is used as the

Table 2. Plating conditions.

Coating sample	Contents		Watts solution (l)	Current density (A dm ⁻²)	Temp. (°C)	pH	Stirring speed (rpm)	Plating time (min)
	Materials	Concentration (g l ⁻¹)						
Ni	—	—	1	2.5	45	4–5	100	90
Ni/GNPs	GNPs	0.3						
Ni/MWCNTs	MWCNTs	0.3						
Ni/GNPs/MWCNTs	GNPs	0.15						
	MWCNTs	0.15						
Ni/GNPs–COOH	GNPs–COOH	0.3						
Ni/MWCNTs–COOH	MWCNTs–COOH	0.3						
Ni/GNPs–COOH /MWCNTs–COOH	GNPs–COOH	0.15						
	MWCNTs–COOH	0.15						



cathode. The plating conditions are shown in table 2. The Ni coatings reinforced with single phase (CNT, GNPs, CNTs–COOH, GNPs–COOH) and hybrid phase (MWCNTs/GNPs, MWCNTs–COOH/GNPs–COOH) were also prepared with the same process to investigate and compare.

2.5. Characterization techniques

Field-emission scanning electron microscopy (FE-SEM, S-4800; Hitachi, Japan) was used to investigate the microstructure of the coatings. FTIR analysis was performed by a SHIMADZU IR Prestige21 Spectrometer. Zeta potential was measured by a Malvern ZS Nano S analyzer. Raman spectra of the coatings were recorded by a LabRAM HR 800 (HORIBA Jobin Yvon, France) using a 532 nm laser source. Optical microscopy was used to measure the thickness of the coatings using an Axiovert 40MAT from Carl Zeiss, Germany. SEM energy dispersive spectroscopy (SEM-EDS) (S-4800; Hitachi, Japan) was used to analyze the composition of the coatings. Microhardness was measured using a microhardness tester (Indenta Met 1106, Buehler, USA) under a load of 10 g for 10 s in the air at room temperature.

3. Results and discussion

3.1. Characterization of –COOH functionalized GNPs and MWCNTs

Carbon nanomaterials including GNPs and MWCNTs have low density, high specific surface area, which tend to the formation of the GNPs and MWCNTs clusters in solutions. FESEM images of as-received GNPs and MWCNTs were shown in figures 2(a) and (b). Some large clusters were observed that resulted from the π - π stacking interaction between two aromatic rings in the graphite structure of GNPs and CNTs. In order to limit the π - π stacking interaction, GNPs and MWCNTs were functionalized with –COOH groups on the surface to create the polarization in the solvents. Figures 2(c) and (d) show GNPs–COOH and MWCNTs–COOH uniformly dispersed on the SiO₂ surface without any clusters. In the functionalization process, the mixture of HNO₃ and H₂SO₄ is a strong oxidizing agent that generated the covalent bonds with the carbon atoms to form the –COOH functional groups on the surface of GNPs and MWCNTs.

FTIR method was performed to confirm the presence of the –COOH functional groups on the surface of GNPs and MWCNTs. Figures 3(a) and (b) show FTIR spectra of GNPs–COOH and MWCNTs–COOH. The band around 3400 cm⁻¹ of wavenumber shows the O–H stretching vibrations of residual water. The band at 1720 cm⁻¹ is assigned to the C=O bonding in the COOH functional group. In addition, the peaks appear at 1365 cm⁻¹ and 1080 cm⁻¹ are assigned to O–H bonding and C–O stretching vibrations mode in the COOH group. [25]. The peak at 1630 cm⁻¹ indicates the C=C bonding of carbon atoms in the graphitic structure of GNPs and MWCNTs which appears in all of the FTIR spectra (figure 3) [25–28]. There are no peaks of the –COOH functional groups detected in as-received GNPs and MWCNTs.

Raman analysis was performed to evaluate the change in the graphitic structure of GNPs and MWCNTs after the functionalization process. Figure 4 shows the Raman spectra of GNPs, MWCNTs, GNPs–COOH, and MWCNTs–COOH. As can be seen, the spectra emerge G peak at 1580 cm⁻¹ which assigned to the graphite structure, the 2D peak at 2670 cm⁻¹ is the characterization peak of the sp² hybridization structure of GNPs, there is no defect peak (D at 1340 cm⁻¹) found in GNPs. For MWCNTs, D peak was observed, that means there are some structural defects or existed some amorphous carbon in MWCNTs [29–31]. For GNPs–COOH and MWCNTs–COOH, the appearance of D peak of GNPs–COOH and the increase of D peak intensity of MWCNTs–COOH indicated the formation of the defects in GNPs and MWCNTs. This is attributed to the

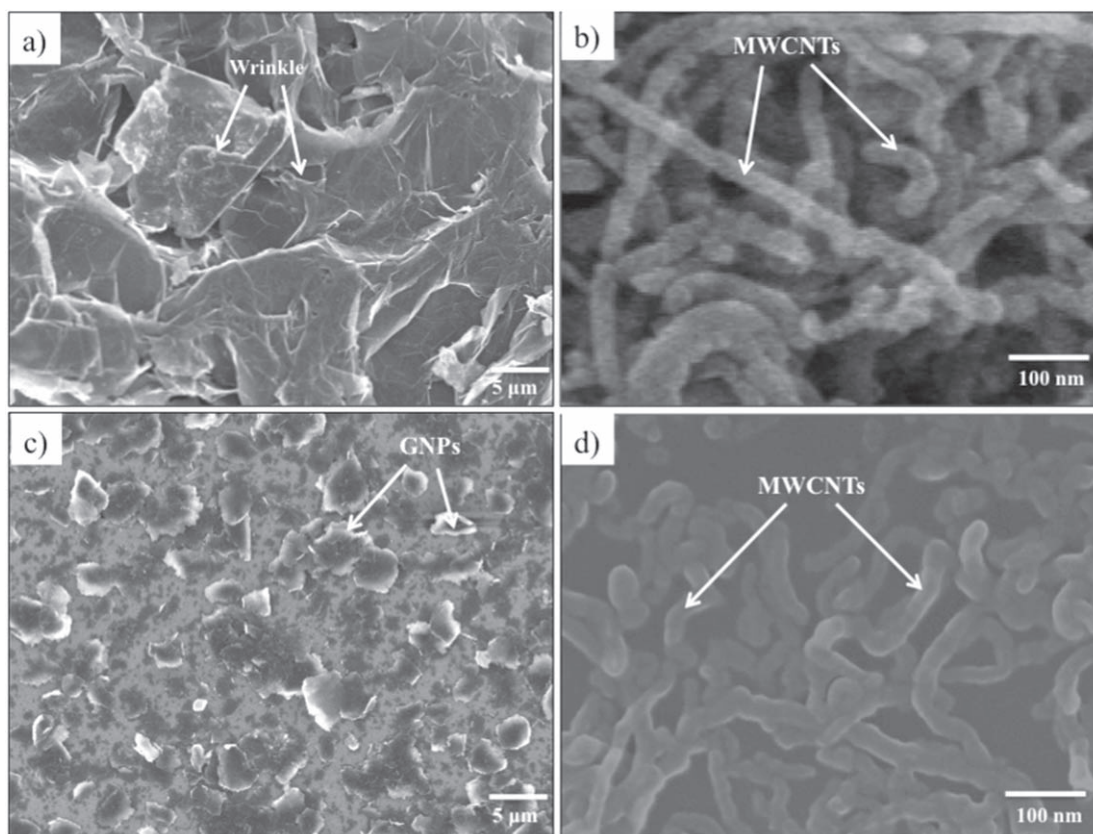


Figure 2. FESEM images of (a) GNPs, (b) MWCNTs (c) GNPs-COOH, (d) MWCNTs-COOH on SiO₂ substrate.

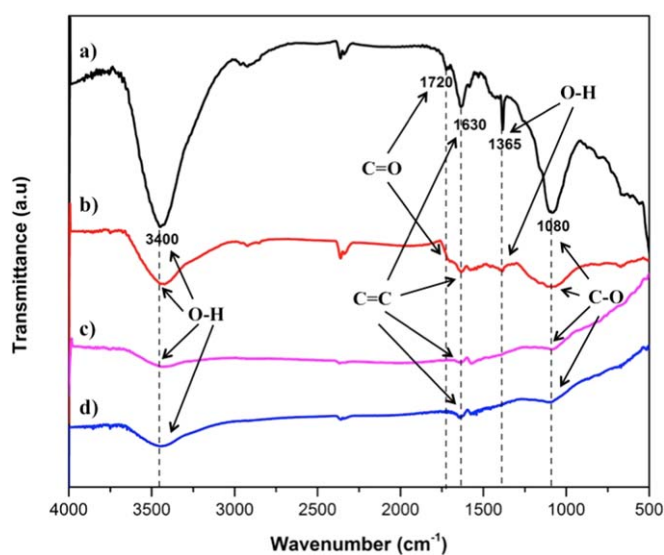


Figure 3. FTIR spectrum of (a) GNPs-COOH, (b) MWCNTs-COOH, (c) MWCNTs, (d) GNPs.

reaction of π orbitals transforming sp^2 into sp^3 hybridization to form the links between graphene and functional groups lead to the defects in the graphitic structure of carbon nanomaterials [32–35].

3.2. The stability of the solutions containing GNPs-COOH and MWCNTs-COOH

Zeta potential was used to evaluate the stability of GNP-COOH as well as MWCNTs-COOH in solution. It is well-known that the absolute Zeta potential value range of 0–15 mV, the suspension is at the little or no stability state; the value of 15–30 mV, the suspension has some stability state but settling lightly. For the value from 30 to 45 mV, the suspension is at the moderate stability. The suspension is at the good stability state when the zeta

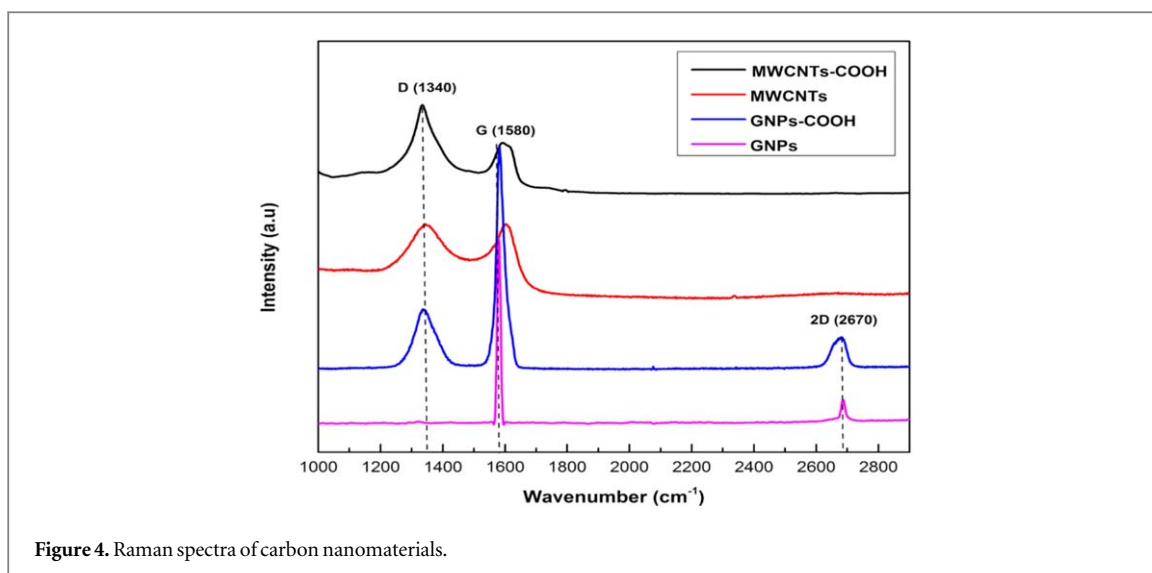


Figure 4. Raman spectra of carbon nanomaterials.

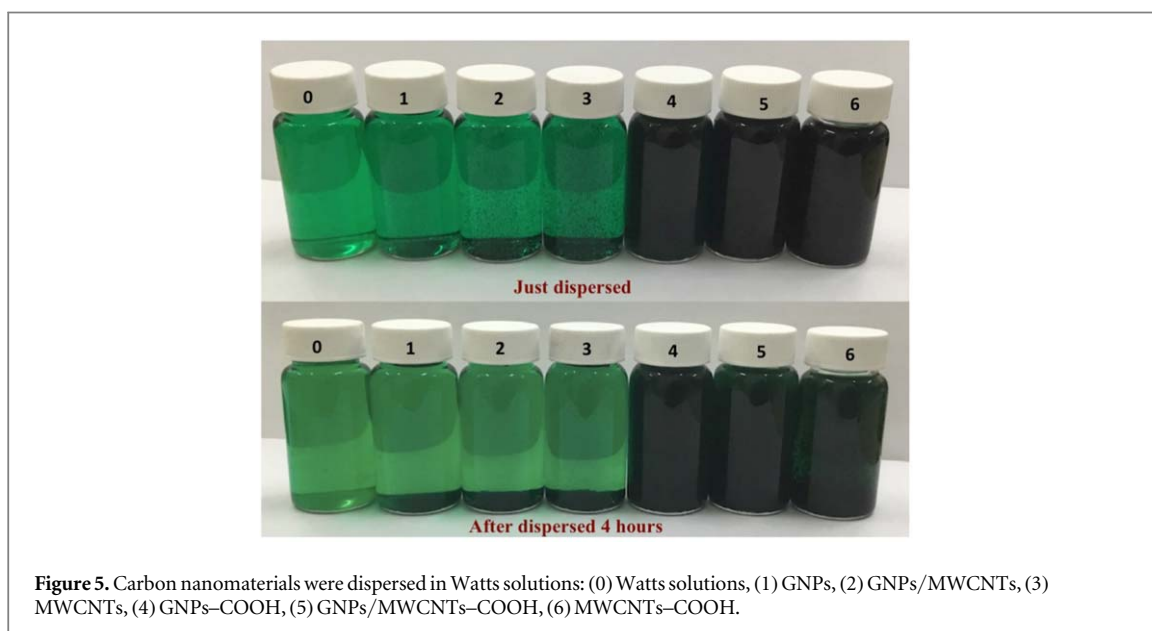


Figure 5. Carbon nanomaterials were dispersed in Watts solutions: (0) Watts solutions, (1) GNPs, (2) GNPs/MWCNTs, (3) MWCNTs, (4) GNPs-COOH, (5) GNPs/MWCNTs-COOH, (6) MWCNTs-COOH.

potential ranges from 45 to 60 mV but it's possible settling when the potential is over the 60 mV, the suspension is at the very good stability state [36–38]. In this study, the absolute zeta potential of GNPs-COOH and MWCNTs-COOH in distilled water was determined to be 27 mV and 23.9 mV respectively. These value indicated that GNPs-COOH and MWCNTs-COOH solutions are stable and could be applied for Watts solution to investigate the reinforcement ability of the Ni coating. Figure 5. shows the dispersion ability of carbon nanomaterials in Watts solution which just dispersed and after dispersed 4 hours. As can be seen, the functionalized carbon nanomaterials showed better stability compared to the non-functionalized carbon nanomaterials in Watts solutions. In addition, the stability of GNPs-COOH is higher than the stability of MWCNTs-COOH and GNPs/MWCNTs-COOH in Watts solutions. It is noted that the plating time is only 90 min and thus the stability of GNPs-COOH and MWCNTs-COOH in Watts solutions could completely satisfy for the electrodeposition process that allows uniform dispersion of carbon nanomaterials in Ni matrix.

3.3. Microstructure of the coatings

Figures 6(b) and (c) show the microstructure of Ni/GNPs and Ni/GNPs/MWCNTs. Some large clusters of GNPs and MWCNTs were observed on the surface. This indicated that GNPs and MWCNTs were not uniformly dispersed in the coatings. Besides, the coatings seem to be having high porosity compared to the bare Ni coating (figure 6(a)). The obtained results may due to the low dispersion ability of as-received GNPs and MWCNTs in Watts solution. In contrary, the Ni coatings reinforced by the functionalized carbon nanomaterials, GNPs-COOH and MWCNTs-COOH were intercalated and uniformly dispersed into the Ni

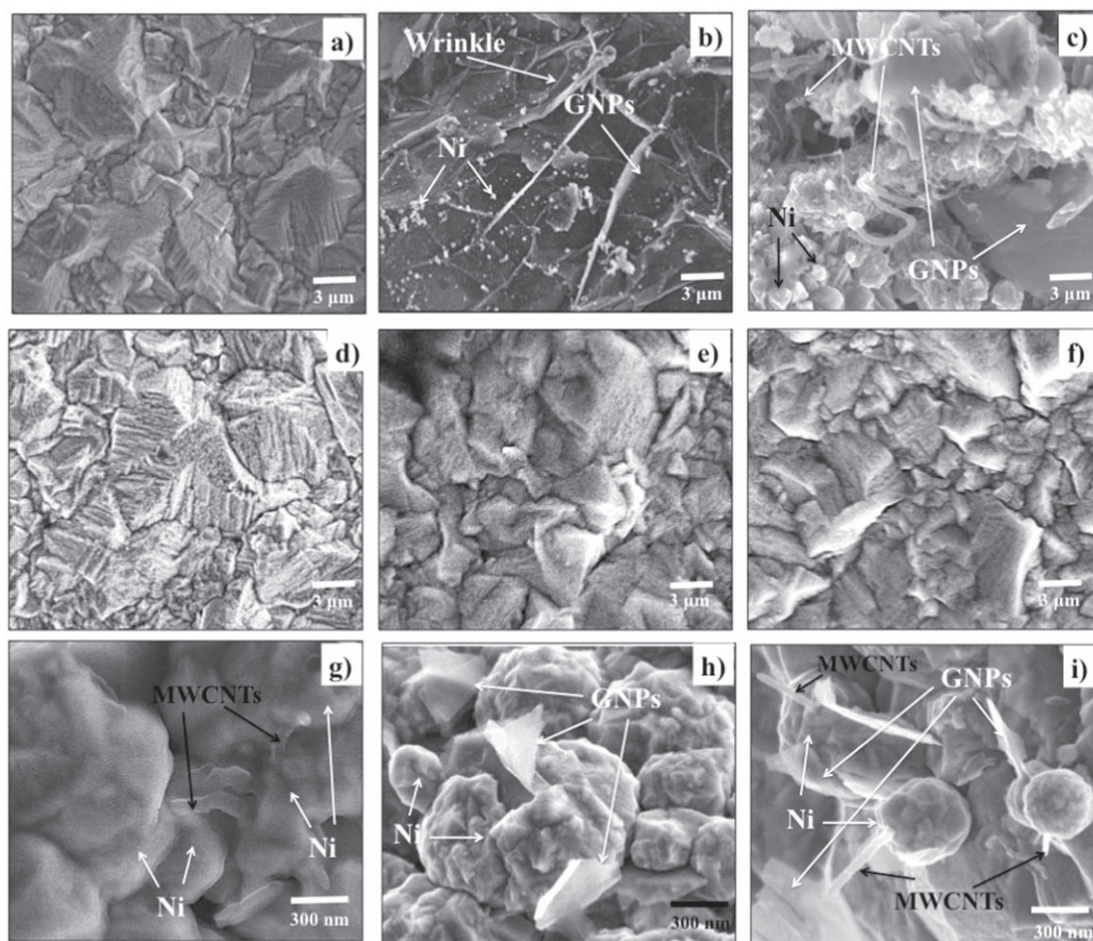


Figure 6. The characterized FESEM image of the coatings: (a) Ni, (b) Ni/GNPs, (c) Ni/MWCNTs, (d) Ni/MWCNTs-COOH, (e) Ni/GNPs-COOH (f) Ni/GNPs/MWCNTs-COOH, and the high-resolution FESEM image of coatings: (g) Ni/MWCNTs-COOH, (h) Ni/GNPs-COOH, (i) Ni/GNPs/MWCNTs-COOH.

matrix, and there are no carbon nanomaterial clusters observed on the surface of the coatings (figures 6(g)–(i)). In addition, the coating surface with the high tightness has smaller grain sizes than the bare Ni coating. This is attributed to the uniform dispersion of the functionalized carbon nanomaterials in Watts solution as discussed in the previous section.

The influence of the composition of the carbon nanomaterials on the surface morphology of the coatings was also observed. Figures 6(d)–(f) show the grain size variation of Ni/MWCNTs-COOH coating, Ni/GNPs-COOH coating, and Ni/GNPs/MWCNTs-COOH coating, respectively. Figures 6(g) and (h) revealed that GNPs-COOH plays the role in preventing the formation of the oriented crystals because of the large size (several microns), whereas MWCNTs-COOH with the small diameter (several dozen of the nanometer) which is easy to intercalate into Ni matrix via the crystal nucleation mechanism along the carbon nanotubes (figure 6(g)). That is why the Ni coating using the GNPs-COOH reinforcements has smaller grain sizes than the Ni/MWCNTs-COOH coating. In order to incorporate the role of GNPs-COOH in hindering the oriented crystal growth and the role of MWCNTs-COOH in the crystal nucleation, the Ni coating reinforced the carbon nanomaterial including both GNPs-COOH and MWCNTs-COOH was fabricated in the same conditions. This incorporation reduced the grain size of the Ni/GNPs/MWCNTs-COOH coating (figure 6(f)). This is attributed to the presence of both GNPs-COOH and MWCNTs-COOH lead to the crystal nucleation and the prevention of the oriented crystal growth of Ni crystalline occurs at the same time (figure 6(i)). Hence, the grain size of Ni/GNPs-COOH/MWCNTs-COOH coating is reduced significantly compared to the Ni/GNPs-COOH coating and Ni/MWCNTs-COOH coating. We performed the thickness measurement on the cross-section of the pure Ni coating and the Ni coatings reinforced carbon nanomaterial. Figure 7 shows the cross-sectional images of selected coatings with the thickness of about 33 μm , 32 μm and 30 μm corresponding to the pure Ni, Ni/GNPs/MWCNTs-COOH and Ni/GNPs/MWCNTs coatings, respectively. The decrease in the thickness of the coatings reinforced carbon nanomaterials implied that the carbon nanomaterials caused to decrease the current efficiency in Watts solution. Besides, it is interesting noted that the presence of the functional group (COOH) on

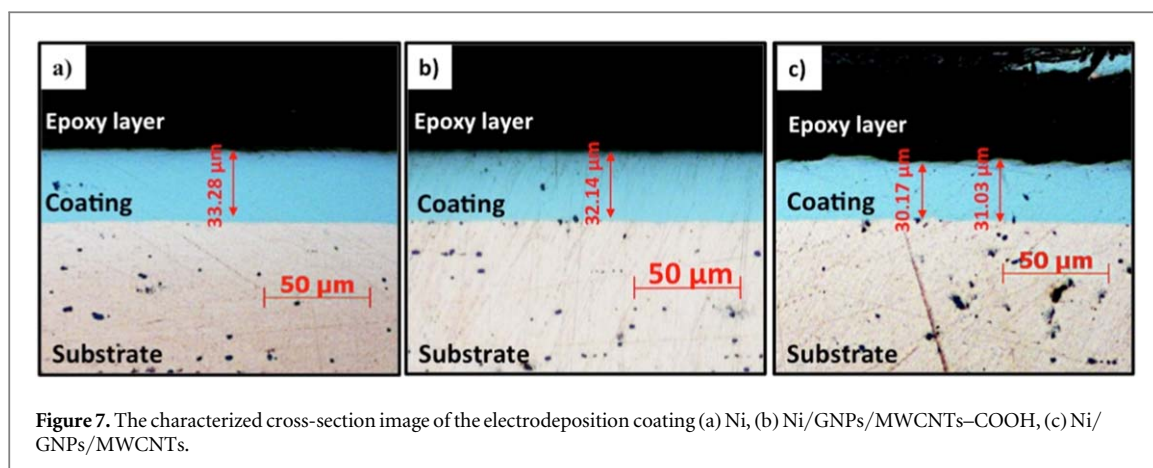


Figure 7. The characterized cross-section image of the electrodeposition coating (a) Ni, (b) Ni/GNPs/MWCNTs–COOH, (c) Ni/GNPs/MWCNTs.

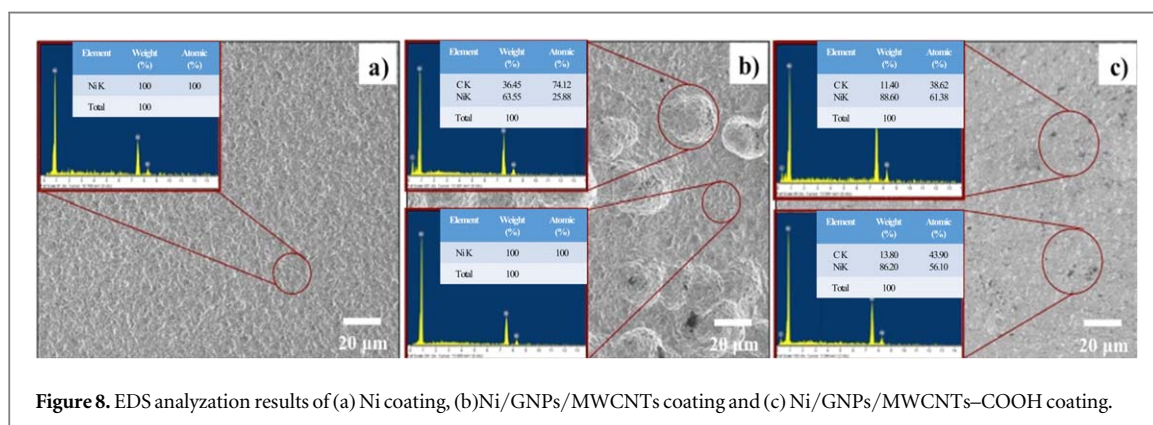


Figure 8. EDS analyzation results of (a) Ni coating, (b) Ni/GNPs/MWCNTs coating and (c) Ni/GNPs/MWCNTs–COOH coating.

the surface of carbon nanomaterials shows a slight enhancement in the current efficiency compared to as-received carbon nanomaterials of the Ni electrodeposition process. In addition, as can be seen in cross-section, the Ni/GNPs/MWCNTs coating surface is rougher than that of the pure Ni coating and the Ni/GNPs–COOH/MWCNTs–COOH coating.

3.4. Content analysis results of the nickel coating reinforced carbon nanomaterials

EDS analysis was used to evaluate the carbon nanomaterial content of the coatings. For the pure Ni coating, EDS result indicates the coating with 100% Ni content in the different positions (figure 8(a)). For the Ni/GNPs/MWCNTs coating, the EDS result changes significantly at different positions. The carbon content occupies about 36.95 wt% at the cluster positions but there is no carbon content detected at other positions which mainly showed 100% Ni content (figure 8(b)). This result demonstrated the non-uniform dispersion in Watts solution leads to the non-uniform dispersion of the carbon nanomaterials in the Ni matrix. The major of carbon nanomaterials were mainly concentrated at clusters and there is no carbon content dispersed at other positions. Figure 8(c) reveals the effectiveness of the functionalized carbon nanomaterials. The EDS spectra show that the carbon content occupies 11.40 wt% on the flat surface of the coating and about 13.80% in the other positions. This demonstrated the carbon nanomaterials were uniformly dispersed in the Ni matrix as using the functionalized carbon nanomaterials

3.5. Influence of the carbon nanomaterials on the microhardness of Ni coatings

Microhardness of the coatings was shown in figure 9. The obtained results revealed that the bare Ni coating has the microhardness of 187 HV, then reduced to 168 HV for Ni/MCNTs coating, 130 HV for Ni/GNPs coating and 154 HV for Ni/GNPs/MWCNTs coating. This demonstrated that using MWCNTs and GNPs without any functional groups (i.e COOH or OH) seem not to be effective in enhancing the microhardness of the coatings. This is attributed to the non-uniform distribution of the carbon nanomaterial which is non-functionalization in Watt solution lead to the non-uniform distribution in the Ni matrix. The carbon nanomaterial component only concentrates at the clusters leading to the porous structure of the Ni coating. This structure reduces significantly the microhardness of the Ni coating. In opposite, using GNPs–COOH and MWCNTs–COOH as reinforcement materials, the microhardness of the coatings increased from 15.2% to 44.7%. Figure 8 reveals that Ni/GNPs–

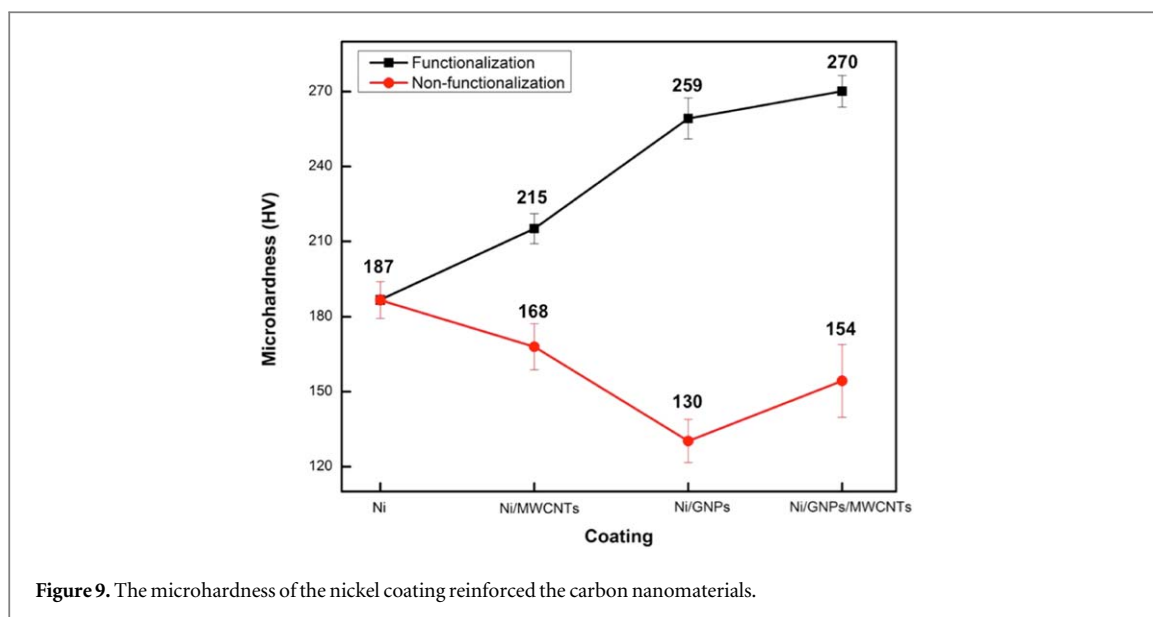


Figure 9. The microhardness of the nickel coating reinforced the carbon nanomaterials.

COOH/MWCNTs–COOH coating has the highest microhardness of 270 HV, whereas the microhardness of the Ni/GNPs–COOH and Ni/MWCNTs–COOH measured to be 259 HV and 215 HV, respectively. The obtained results were attributed to the uniform dispersion of both MWCNTs–COOH and GNPs–COOH in the Ni matrix and the grain refinement effect. This could be explained as the following: the presence of GNPs–COOH and MWCNTs–COOH in the Ni matrix which helps to reduce the grain size of Ni as demonstrated in previous sections. According to the Hall-Petch equation which describes the relationship between the hardness and grain size [39]: $H_V = H_0 + k_H d^{-1/2}$, where H_0 and k_H are constants, d is the grain size. The smaller grains size is, the harder coating is. In other hands, the –COOH functional groups of GNPs–COOH and MWCNTs–COOH are responsible for absorbing the Ni^{2+} ions on the surface of GNPs and MWCNTs in Watts solutions [40]. In the plating process, the GNPs (or MWCNTs) absorbed Ni^{2+} are reduced at the cathode in order to form Ni nanoparticle and bond to the Ni crystal (figure 1), bondings between Ni and carbon nanomaterials lead to the enhancement in the load transfer effect from the Ni matrix to high strength reinforcement materials. The improvements in the coating containing hybrid materials could be attributed to the synergistic strengthening effects of the MWCNTs and GNPs as reported in other studies [41, 42]. In addition, the other strengthening mechanisms such as thermal expansion coefficient mismatch and Orowan looping may also affect the mechanical properties of the coatings, which will be clarified in the future work [43].

4. Conclusions

Ni coatings reinforced functionalized carbon nanomaterials were successfully fabricated in industrial scale by the electrodeposition method. The effect of COOH functional group on the dispersion state of carbon nanomaterials in Watt solution and the microstructure, composition and hardness of the coating was investigated. The microhardness of the Ni coatings reinforced COOH functionalized carbon nanomaterials is much improved in comparison with bare Ni coating and Ni coating containing as received carbon nanomaterials. The Ni coating containing MWCNTs–COOH/GNPs–COOH hybrid material had the highest microhardness of 270 HV and improved up to 44.7% compared to bare Ni coating. The enhancement was attributed to the uniform dispersion of carbon nanomaterials, the synergistic strengthening effects of the MWCNTs and GNPs, the grain refinement of the Ni matrix and the load transfer effect.

Acknowledgments

Authors would like to thank the financial support from FIRST under Subproject 37/FIRST/1a/IMS ‘Research on the application of carbon nanomaterials for improving the mechanical properties of industrial electroplating’.

ORCID iDs

Pham Van Trinh  <https://orcid.org/0000-0001-7905-3647>

References

- [1] Tseluikin V N and Koreshkova A A 2014 *Russ J Appl Chem* **87** 1251–3
- [2] Tseluikin V N and Kanaf'Eva O A 2015 *Chem Pet Eng* **51** 54–7
- [3] Liu Z et al 2016 *Lasers Manuf Mater Process* **3** 1–8
- [4] Punith Kumar M K, Singh M P and Srivastava C 2015 *RSC Adv.* **5** 25603–8
- [5] Carpenter C R, Shipway P H and Zhu Y 2011 *Wear* **271** 2100–5
- [6] Shao W et al 2012 *Adv Mat Res* **548** 101–4
- [7] Selvakumar A, Perumalraj R, Sudagar J and Mohan S 2016 *Proc Inst Mech Eng Part L J Mater Des Appl* **230** 319–27
- [8] Novoselov K S et al 2005 *Nature* **438** 197–200
- [9] Lee C, Wei X, Kysar J W and Hone J 2008 *Science* **321** 385–8
- [10] Ovid'Ko I A 2013 *Rev Adv Mater Sci* **34** 1–11
- [11] Dai J F, Wang G J, Ma L and Wu C K 2015 *Rev Adv Mater Sci* **40** 60–71
- [12] Ávila A F and Lacerda G S R 2008 *Mater Res* **11** 325–33
- [13] Wei X-L et al 2008 *Adv Funct Mater* **18** 1555–62
- [14] Kumar C M P, Venkatesha T V and Shabadi R 2013 *Mater Res Bull* **48** 1477–83
- [15] Algul H et al 2015 *Applied Surface Science* **359** 340–8
- [16] Szeptycka B, Gajewska-midzialek A and Babul T 2016 *J Mater Eng Perform* **25** 3134–8
- [17] Jabbar A et al 2017 *RSC Adv* **7** 31100–9
- [18] Singh S, Samanta S, Das A K and Sahoo R R 2018 *Surfaces and Interfaces* **12** 61–70
- [19] Huitao Y, Bangwen Z, Chaoke B, Ruihong L and Ruiguang X 2016 *Scientific Reports* **6** 36143
- [20] Ying W and Zhenyu S 2015 *Current Opinion in Colloid & Interface Science* **20** 311–21
- [21] Tongping Z, Xiaofang Z, Yuwei C, Yongxin D and Jianming Z 2018 *ACS Sustainable Chem Eng* **6** 1271–8
- [22] Koga H, Tonomura H, Nogi M, Suganuma K and Nishina Y 2016 *Green Chem.* **18** 1117–24
- [23] Xiong R, Hu K, Grant A M, Ma R L, Xu W N, Lu C H, Zhang X X and Tsukruk V V 2016 *Adv. Mater.* **28** 1501–9
- [24] Dung N D et al 2008 *J Korean Phys Soc* **52** 1372–7
- [25] Zhang J et al 2003 *J Phys Chem B* **107** 3712–8
- [26] Jang J, Bae J and Yoon S H 2003 *J Mater Chem* **13** 676–81
- [27] Bui H T et al 2014 *J Korean Phys Soc* **65** 312–6
- [28] Pham V T et al 2017 *RSC Adv* **7** 49937–46
- [29] Reina A et al 2009 *Nano Lett* **9** 30–5
- [30] Nguyen V T, Le H D, Nguyen V C, Ngo T T T, Le D Q, Nguyen X N and Phan N M 2013 *Adv Nat Sci Nanosci Nanotechnol.* **4** 035012
- [31] Dong X et al 2011 *Carbon NY* **49** 3672–8
- [32] Liu J et al 2015 *Anal Chim Acta* **859** 1–19
- [33] Haldar S et al 2012 *Solid State Commun* **152** 1719–24
- [34] Niyogi S et al 2010 *Nano Lett* **10** 4061–6
- [35] Mao H Y et al 2013 *Prog Surf Sci* **88** 132–59
- [36] Pham V T et al 2018 *J Mol Liq* **269** 344–53
- [37] Ghadimi A, Saidur R and Metselaar H S C 2011 *Int J Heat Mass Transf* **54** 4051–68
- [38] Ivall J, Langlois-Rahme G, Coulombe S and Servio P 2017 *Nanotechnology* **28** 55702
- [39] Liu X D, Nagumo M and Umemoto M 1997 *Mater Trans JIM* **38** 1033–9
- [40] Tang Y, Yang X, Wang R and Li M 2014 *Mater. Sci. Eng. A* **599** 247–54
- [41] Li Z, Fan G, Qiang G, Zhiqiang L, Yishi S and Di Z 2015 *Carbon* **95** 419–27
- [42] Xiaofeng C, Jingmei T, Yichun L, Rui B, Fengxian L, Caiju L and Jianhong Y 2019 *Carbon* **146** 736–55
- [43] Saboori A, Dadkhah M, Fino P and Pavese M 2018 *Metals (Basel)* **8** 423